

Epoxidized Soybean Oil: Evaluation of Oxidative Stabilization and Metal Quenching/Heat Transfer Performance

Rosa L. Simencio Otero, Lauralice C.F. Canale, Diego Said Schicchi, Eliana Agalioitis, George E. Totten, and Gustavo Sánchez Sarmiento

(Submitted May 31, 2012; in revised form October 23, 2012; published online April 9, 2013)

Vegetable and animal oils as a class of fluids have been used for hundreds of years, if not longer, as quenchants for hardening steel. However, when petroleum oils became available in the late 1800s and early 1900s, the use of these fluids as quenchants, in addition to their use in other industrial oil applications, quickly diminished. This was primarily, but not exclusively, due to their generally very poor thermal-oxidative instability and the difficulty for formulating fluid analogs with varying viscosity properties. Interest in the use of renewable fluids, such as vegetable oils, has increased dramatically in recent years as alternatives to the use of relatively non-biodegradable and toxic petroleum oils. However, the relatively poor thermal-oxidative stability has continued to be a significant reason for their general non-acceptance in the marketplace. Soybean oil (SO) is one of the most highly produced vegetable oils in Brazil. Currently, there are commercially produced epoxidized versions of SO which are available. The objective of this paper is to discuss the potential use of epoxidized SO and its heat transfer properties as a viable alternative to petroleum oils for hardening steel.

Keywords epoxidized soybean oil, heat transfer, quenching

1. Introduction

Hardening steel occurs by first heating the steel to the specified austenitizing temperature, typically in the range of 750–1100 °C, and cooling it in such a way that the desired microstructure is formed obtaining required properties such as hardness, strength, and toughness. The main objective of any quenchant is to produce the desired metallurgical transformations. In addition, the quenchant must prevent cracking and minimize distortions due to non-uniform heat transfer over the surface of the steel.

The microstructures that are formed during quenching depend on the heat transfer properties at the hot metal interface. The cooling time-temperature pathway is designated as the cooling curve. One method of illustrating the steel transformation microstructures during the quenching process is to superimpose the cooling time-temperature curve for steel cooled in a specific quenching medium over a time-temperature-

transformation (TTT) or continuous-cooling-transformation (CCT) curve for the steel of interest.

The most common quenchants, depending on the steel and hardening process, include air, petroleum oil, water, brine, aqueous polymer solutions, and high-pressure gas quenching. Of the vaporizable quenchants, petroleum oil-derived fluids are the most commonly encountered throughout the industry.

The challenge to replace petroleum basestocks due to potential problems with long-term availability in addition to the relative toxicity and poor biodegradability has proposed the vegetable oils as interesting alternative because of their biodegradable, environmentally friendly, and non-toxic renewable basestocks. Beyond these characteristics, vegetable oil have good anti-friction properties, low volatility, high viscosity index (VI), and good miscibility with other fluids (Ref 1). Although the potential use of vegetable oils as basestocks for industrial oil formulation continues to be of interest, they possess a number of very substantial limitations, not the least of which is relatively poor thermal-oxidative stability relative to petroleum oil-derived formulations. For example, vegetable oils typically cannot withstand reservoir temperatures in excess of 80 °C due to the onset of oxidation, although the use of antioxidants can partially offset this notable limitation (Ref 2, 3). Oxidation limits the useful life of vegetable oil-derived fluids because of the increased viscosity, which is further accelerated by elevated temperatures and contact with metals such as iron and copper (Ref 4). Adhvaryu et al. (Ref 5) have concluded that soybean oil (SO) oxidizes at a rate that is at least an order of magnitude greater than that of petroleum oil.

The thermo-oxidative stability of a vegetable oil is dependent on the fatty ester composition of the triglyceride structure. Increasing amounts of unsaturation in the fatty ester structure lead to increased oxidative instability. Schneider (Ref 6) and

Rosa L. Simencio Otero and Lauralice C.F. Canale, Escola de Engenharia de São Carlos, Universidade de São Paulo, São Carlos, SP, Brazil; Diego Said Schicchi, Centro de Mecánica, Instituto Nacional de Tecnología Industrial, Buenos Aires, Argentina; Eliana Agalioitis, Consejo Nacional de Investigaciones Científicas y Técnicas (CONICET), Buenos Aires, Argentina; George E. Totten, Department of Mechanical and Materials Engineering, Texas A&M University, Seattle, WA; Gustavo Sánchez Sarmiento, Facultad de Ciencia y Tecnología, Universidad del Salvador, Buenos Aires, Argentina; and Facultad de Ciencia y Tecnología, Universidad Austral, Buenos Aires, Argentina. Contact e-mail: rosa_simencio@yahoo.com.br.

Kodali (Ref 7) have reported that the relative rate of oxidation increases as the number of double bonds in conjugation with each other increases in the following relative order: stearic (1) < oleic (10) < linoleic (100) < linolenic (200), shown in Fig. 1.

Knothe (Ref 8) reported that the initiation step of oxidative degradation involves hydrogen abstraction from fatty ester of the lipid by an initiator. The most favored position for hydrogen abstraction occurs with the lowest activation energy which is an allylic methylene, the (CH₂) adjacent to the CH=CH moiety, and the allylic radical that is formed is stabilized by resonance over the double bond structure and the resonance stabilization increases with the number of double bonds in conjugation. Bis-allylic positions in polyunsaturated fatty acids such as linoleic acid (double bonds at Δ9 and Δ12, giving one bis-allylic position at C-11) and linolenic acid (double bonds at Δ9, Δ12, and Δ15, giving two bis-allylic positions at C-11 and C-14) are even more prone to autoxidation than the allylic position of oleic acid as indicated in Fig. 1.

Souza et al. (Ref 9) reported that although selection of the most effective antioxidants does provide substantially improved inhibition to oxidation, this is insufficient to rival the oxidative stability possible with the use of petroleum oil-based fluids. Clearly, something significantly more effective is needed to provide the necessary oxidative stability for applications where the fluid will be subjected to relatively high, even if only for a short time, thermal excursions.

Others possibilities to improve the thermo-oxidative stability of the vegetable oils are genetic and chemical modification. Modification of the chemical structure of vegetable oils has been proposed for the development of environmental friendly vegetable oil-derived basestocks. One modification of the vegetable oil structure that has proposed is epoxidation. Figure 2 (Ref 10) provides a generic illustration of a fully epoxidized soybean oil (ESBO). Double bond epoxidation has been utilized for over 50 years as described by Julian et al. (Ref 11) and Findley et al. (Ref 12). Epoxidized vegetable oils are of potentially great interest for commercial applications as lubricants, synthetic detergents, and for the production of polyurethane foams.

Wu et al. (Ref 13) showed that epoxidized rapeseed oil exhibited greater oxidative stability than unepoxidized rapeseed oil without chemical modification. Moreover, the epoxidation treatment did not modify the biodegradability of the basestock.

Adhvaryu and Erhan (Ref 1) and Erhan et al. (Ref 14) reported that ESBO demonstrated improved thermal and oxidative stability relative to unepoxidized SO and genetically

modified high oleic SO in certain high temperature lubricant applications.

Epoxidation has been shown to significantly improve oxidative stability relative to unepoxidized triglyceride structure. Only limited data are available comparing the resulting oxidative stability of the epoxidized triglycerides with their functionally equivalent petroleum oil basestocks.

The objective of this paper is to discuss recently obtained results showing the dramatic improvement in thermal-oxidative stability of ESBO and to discuss their potential use and heat transfer properties as viable alternatives to petroleum oils for hardening steel.

2. Experimental Procedures

The ESBO used in this work was obtained from Inbra (Indústrias Químicas Ltda) and was designated as ESBO. The SO, produced by Cargill Agrícola S/A, was purchased at a local market in São Carlos/SP, Brazil, and was commercially designated as Liza and classified as “pure” SO. In addition, one Fatty Acid Methyl Ester (FAME) derivative of soybean soapstock designated as FAME 3P was obtained from Cognis do Brasil Ltda. (SO soapstock is a by-product of the caustic refining process of SO.) A reaction schematic illustrating the general synthesis of FAME from a triglyceride such as SO is shown in Fig. 3. The FAME 3P was added with stirring into ESBO, producing the formulations designated in Table 1.

The two fully formulated, commercially available, petroleum-based quench oils used for comparison were Lubrifort Temp 4 (conventional “slow” oil) and Lubrifort Temp 2 (accelerated “fast” oil). These petroleum-based quench oils

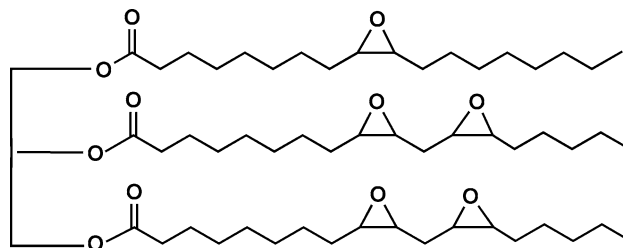


Fig. 2 Generic simplified illustration of one potential component in ESBO, adapted from Hwang and Erhan (Ref 10)

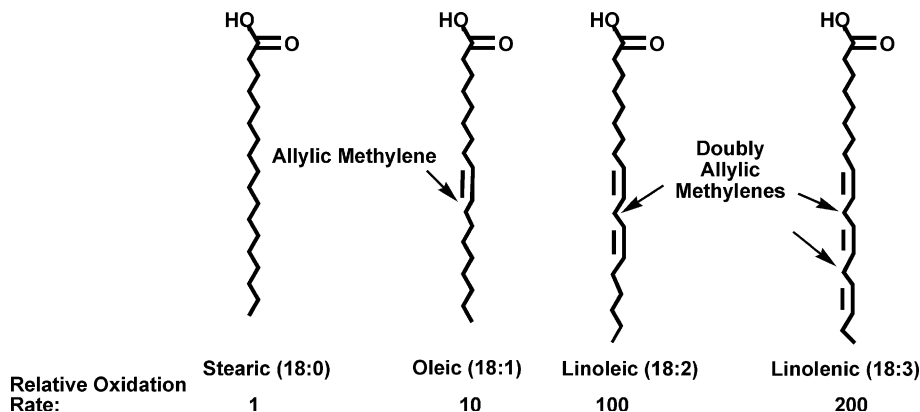


Fig. 1 Allylic methylene functionality: 18:3 > 18:2 > 18:1

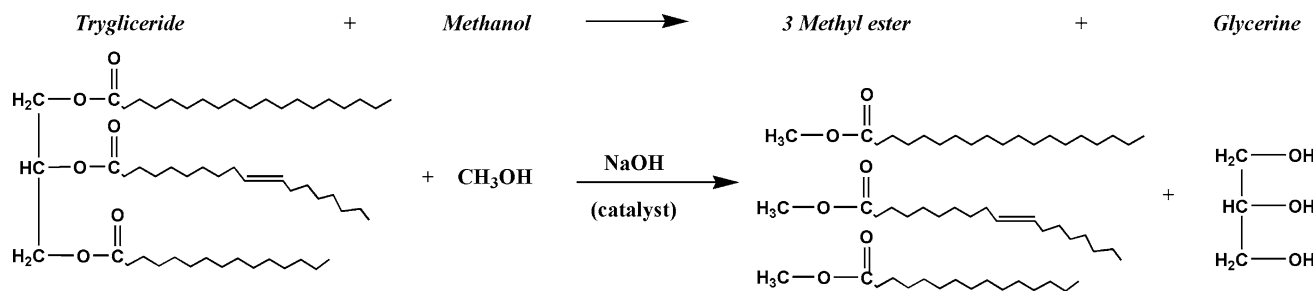


Fig. 3 General illustration of the synthesis of a FAME derivative from a triglyceride

Table 1 ESBO and FAME formulations using for thermal-oxidation study

Designation	% ESBO	% FAME
ESBO	100	0
EF 30	70	30
EF 38	62	38
EF 60	40	60
FAME	0	100

were obtained from Quimifort Indústria e Comércio Ltda., São Carlos, SP, Brazil.

Viscosity was measured at 40 and 100 °C using calibrated Cannon-Fenske viscometer tubes according to ASTM D445-06 “Standard Test Method for Kinematic Viscosity of Transparent and Opaque Liquids (and Calculation of Dynamic Viscosity).” The VI was calculated according to ASTM D2270-10 “Standard Practice for Calculating Viscosity Index from Kinematic Viscosity at 40° and 100°C.” All viscosity measurements were run in duplicate and the average value was reported.

Cooling curves were obtained at a 60 °C non-agitated condition, according to ASTM D6200 “Standard Test Method for Determination of Cooling Characteristics of Quench Oils by Cooling Curve Analysis.” This method utilizes a 12.5-mm-dia × 60-mm INCONEL 600 cylindrical probe with a Type K thermocouple inserted into the geometric center. After heating the probe in a furnace to 850 °C, it was manually and rapidly immersed into 2000 mL of the oil to be tested which was contained in a tall-form stainless steel beaker. The probe temperature and cooling times were recorded at selected time intervals to establish a cooling temperature versus time curve. All measurements were performed in duplicate and averaged. The averaged data are reported here.

3. Results and Discussion

3.1 Viscosity Properties

The viscosity-temperature relationship is an important physical property for any potential basestock that may be used for steel quenchant formulations since heat transfer is exponentially related to the viscosity of the heat transfer medium. As steel cools, the viscosity at the interface between the cooling metal surface and the bulk fluid decreases and the interfacial heat transfer coefficient which is partly determined by the structurally dependent, viscosity-temperature relationship of the basestock will control the time-temperature (cooling curve)

exhibited by the quenchant which, in turn, controls the overall hardening properties of the quenching medium. According to Santos et al. (Ref 15), the viscosity of the triglyceride components of the vegetable oil increases with the fatty acid ester chain length and decreases with the amount of unsaturation in the fatty acid ester alkyl chain.

The results of kinematic viscosity measurements and the calculated VI obtained for each formulation and the two petroleum oil quenchants are shown in Table 2. The viscosity of ESBO, at both temperatures, is higher than the other formulations and as reported in a previous study described in the literature (Ref 1). FAME exhibited the lowest viscosity compared with the other formulations, as expected since it is a relatively low molecular weight monoester. Also, increasing amounts of FAME addition to the ESBO resulted in a progressive viscosity decrease. The reason for performing this study was to examine the potential use of FAME addition to decrease the otherwise extraordinarily high viscosity of ESBO which would inhibit its potential use as a quenchant. These data show that, as expected, the addition of FAME to ESBO can be performed to obtain reasonably similar viscosity properties relative to unadulterated SO. However, the viscosity data of the ESBO/FAME blends do not compare well with either petroleum oil quenchant evaluated.

The viscosity of the slow oil was considerably greater than either the SO or most of the ESBO blends. The viscosity of the fast oil was substantially lower than either the slow oil or SO. The viscosities of the EF 60 blend were similar to the fast petroleum oil quenchant (Temp 2) at 40 °C, and the viscosity of EF 30 blend approximated the slow petroleum oil quenchant (Temp 4). Interestingly, while it is possible to blend ESBO/FAME to obtain the viscosity of either the fast or the slow oil at 40 °C, it is not possible to match the viscosities at both 40 and 100 °C.

The reason for the inability to match the viscosity properties of these blends with the petroleum oil quenchants is the substantially different VI properties of these fluids. Table 2 shows that the VI of SO (229) was significantly higher than either the fast (143) or the slow (99) petroleum oil and the VI of the fast oil was nearly 50% greater than that of the slow oil. These values represent the expected change in viscosity of the oil with change in temperature, and the lower the VI value, the greater the change that is expected. FAME had the highest VI (347) of the fluids evaluated, even greater than SO, and the value for ESBO (141) was similar to that published previously (142) (Ref 16). Increasing amounts of FAME in an ESBO/FAME blend resulted in a progressively increasing VI. It should be noted that a comparison of the viscosity properties of the fast and slow petroleum quench oils indicates that the basestocks

Table 2 Kinematic viscosity and VI determined for every formulation and petroleum oil-based quenchant

Physical property	SO, ESBO, FAME and ESBO/FAME blends						Petroleum oil quenchant	
	SO	ESBO	EF 30	EF 38	EF 60	FAME	Slow oil Temp 4	Fast oil Temp 2
Viscosity, cSt at 40 °C	31.71	162.77	48.65	37.43	16.25	4.76	52.86	16.96
Viscosity, cSt at 100 °C	7.74	19.91	9.48	8.11	4.57	2.02	7.38	4.05
VI	229	141	183	199	220	347	99	143

are different for these two oils. The slow oil possesses a substantially greater fluid viscosity which would be expected to result in generally slower cooling rates throughout the quenching process relative to the fast oil since heat transfer decreases with increasing viscosity.

3.2 Quenching/Heat Transfer Performance

Quenching cooling times and cooling rates and heat transfer coefficients for each fluid evaluated in this work were determined by cooling curve analysis under unagitated conditions according to ASTM D6200 at a bath temperature of 60 °C. Two petroleum-based quenchants were used for comparison: Lubrifort Temp 2 (fast oil) and Lubrifort Temp 4 (slow oil). The “slow” and “fast” oil designations typically refer to the film boiling/nucleate boiling properties of a quenchant. When hot (≈ 850 °C) steel (or Inconel) is immersed into a vaporizable fluid such as a petroleum oil, the hot surface is surrounded by a vapor blanket and heat transfer occurs by a full-film boiling mechanism. Heat transfer through this vapor blanket is typically the slowest encountered in the process. Upon further cooling, the film collapses and results in nucleate boiling. The transition between full-film boiling and nucleate boiling is designated as the Leidenfrost temperature and heat transfer is typically fastest in this region. When the temperature decreases to a temperature less than the boiling point of the components of the oil, heat transfer occurs predominantly by convection which is considerably slower than nucleate boiling, but faster than full-film boiling. “Fast” quench oils typically contain additives that facilitate the rupture of the vapor blanket.

Since nucleate boiling is facilitated at a higher temperature (shorter time), such oils are used to harden otherwise difficult to harden steels such as carbon steels and low-hardenability alloy steels. Because nucleate boiling occurs sooner than would be observed for a slow oil (with otherwise identical composition and physical properties), it is designated as a “fast” quenching oil. Figures 4 and 5 show the cooling time-temperature curves and cooling rate curves for the fluids evaluated as part of this work. The cooling curve parameters for the fluids evaluated in this work are summarized in Table 3.

The first comparison to be discussed is for the “fast” and “slow” petroleum oil. When evaluating these results, it is important to consider the viscosity and VI relationships shown in Table 2 which suggest that these two quench oils are formulated using substantially different basestock, with the “fast” quench oil (Temp 2) being formulated with a relatively low viscosity (16.06 cSt) versus 52.86 cSt viscosity for the “slow quench oil (Temp 4). This complicates the cooling curve comparison of the two quench oils. Table 3 shows that the cooling rate at the higher 700 °C temperature ($CR_{700^{\circ}C}$) is much faster for the slow oil and the time to cool to 700 °C ($t_{700^{\circ}C}$) is somewhat faster. Furthermore, the cooling time-temperature and

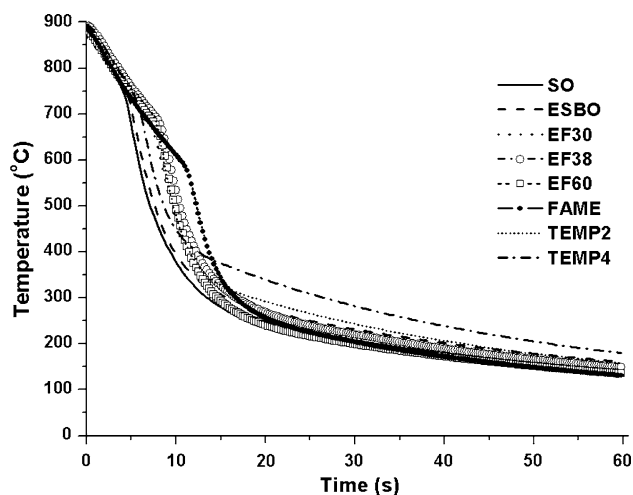


Fig. 4 Cooling curves data at 60 °C bath temperature with no agitation

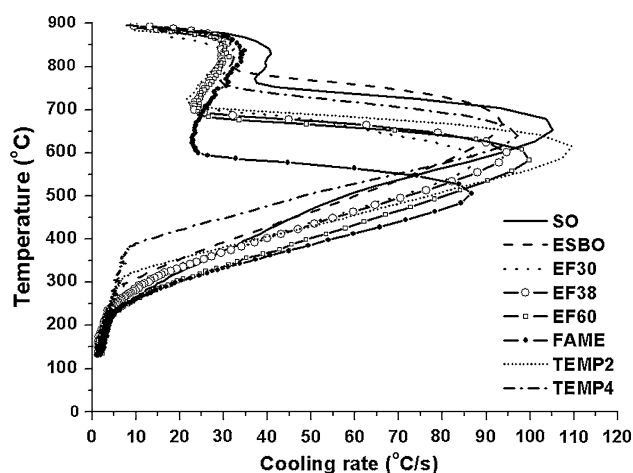


Fig. 5 Cooling rates' data at 60 °C bath temperature with no agitation

cooling rate curves do not exhibit the substantially reduced full-film boiling region more conventionally expected for fast oil compared to a slow quenching oil. In fact, the slow quenching oil, even at the higher viscosity, did not exhibit the expected extended full-film boiling. The cooling rate at 300 °C ($CR_{300^{\circ}C}$) was essentially equivalent for both oils. However, the cooling times to 300 ($t_{300^{\circ}C}$) and 200 °C ($t_{200^{\circ}C}$) are substantially slower for the slow quench oil relative to the fast oil, which is the expected behavior.

The next comparison to be performed relative to the fast and slow petroleum oil quenchants is SO. Inspection of the SO

Table 3 Cooling parameters obtained by ASTM D6200 at 60 °C bath temperature and with no agitation

Cooling curve parameters obtained at 60 °C bath temperature	SO, ESBO, FAME and ESBO/FAME blends						Petroleum oil quenchant	
	SO	ESBO	EF 30	EF 38	EF 60	FAME	Slow oil Temp 4	Fast oil Temp 2
CR _{700°C} , °C/s	94.87	90.35	27.47	23.26	24.23	25.53	74.96	32.98
CR _{300°C} , °C/s	15.60	8.18	11.89	12.90	18.97	19.31	5.50	5.81
CR _{200°C} , °C/s	3.00	3.03	2.67	2.77	3.32	3.57	2.98	2.70
<i>t</i> _{700°C} , s	4.80	5.14	6.58	7.47	6.82	6.29	6.08	7.37
<i>t</i> _{300°C} , s	13.53	15.83	16.31	16.80	14.66	16.70	23.22	18.72
<i>t</i> _{200°C} , s	28.94	40.64	28.94	36.22	29.84	31.15	51.78	42.20

cooling time-temperature and cooling rate curves, shows that it does exhibit a minimal vapor blanket cooling region which typically accompanies full-film boiling. However, the cooling curve parameters for SO in Table 3 show that it exhibits substantially faster values for both CR_{700°C} and *t*_{700°C} relative to either petroleum oil quenchant, suggesting that the cooling process for SO is probably predominated by convection. The CR_{300°C} and *t*_{300°C} are also much faster than either the fast or slow oil. While the CR_{200°C} and *t*_{200°C} are also faster than either petroleum oil, the difference is considerably less. Overall, the SO is clearly the fastest of the quenchants evaluated.

When comparing the cooling time-temperature and cooling rate curves for FAME (which is the methyl ester of fatty acid components derived from methanolysis of SO), it is important to realize that FAME is composed of monoesters which represent a much lower molecular weight, and consequently is correspondingly more volatile than SO which is a triglyceride (triester). A comparison of the cooling time-temperature curve and cooling rate curve for FAME shows that it exhibits a substantially longer vapor blanket (full-film boiling) region than either SO or either petroleum oil quenchant. The data in Table 3 show that the CR_{700°C} is much slower than SO and the cooling rates at CR_{300°C} and CR_{200°C} are faster than SO, although the differences may not be significant. Although the cooling rate 700 °C is slower due to the full-film boiling process, the cooling rates at 300 and 200 °C are faster for FAME than those exhibited by either the fast or the slow petroleum oil. The cooling time at 700 °C is very similar for FAME and the petroleum oil quenchants, although the cooling times are faster for FAME at 300 and 200 °C.

The CR_{700°C} for ESBO is approximately the same as SO and, like SO, it exhibits a very minimal apparent vapor blanket region. In view of the expected very high boiling points for both SO and ESBO and the corresponding low vapor pressure, it is likely that the cooling process for ESBO is also predominated by convection. The CR_{300°C} is much less for ESBO than SO, which is likely due to the much higher viscosity of ESBO (162.8 cSt) compared to SO (31.7 cSt). The *t*_{700°C} and *t*_{300°C} are slightly longer for ESBO than SO, although the *t*_{200°C} is much longer for ESBO. Compared to FAME, the CR_{700°C} is much faster because FAME exhibits a prolonged vapor blanket cooling region which is not observed for ESBO. The *t*_{700°C} and *t*_{300°C} are faster for ESBO, but ESBO has a longer *t*_{200°C}. ESBO cools much faster to 700 °C than either petroleum oil and is also faster at 300 °C, although it is only marginally faster at 200 °C. The *t*_{700°C} and *t*_{300°C} are faster for ESBO than either petroleum oil. Although the *t*_{200°C} is faster for

ESBO than the slow petroleum oil, the values for *t*_{200°C} are approximately comparable for ESBO and the fast petroleum oil.

The reason for doing this work was to determine if it is possible to reasonably match the quenching performance of a petroleum oil, whether fast or slow, or both, by blending FAME and ESBO. The approach used to address this question was to blend different ratios of FAME and ESBO and compare the quenching properties with the fast and slow petroleum oil quenchants used for this study. Careful inspection of the cooling time-temperature and cooling rate curves shows that the vapor blanket cooling region was significantly extended relative to SO and ESBO, but somewhat less than that observed for FAME. However, the vapor blanket regions exhibited by EF 30, EF 38, and EF 60 were intermediate between FAME and ESBO, but quite similar to each other. The CR_{700°C} of the FAME and EF 30, EF 38, and EF 60 blends were comparable and were also slower than ESBO and both the fast and slow petroleum oil. The CR_{300°C} followed the trend

$$\text{ESBO} < \text{EF 30} < \text{EF 38} < \text{EF 60} < \text{FAME}$$

This trend was directly proportional to decreasing fluid viscosities. No similar identifiable trend was observed for CR_{200°C}. In addition, none of the cooling times followed any significant trend. Finally, and importantly, none of the ESBO/FAME blends produced cooling curve time and rate parameters that matched well with the fast and slow petroleum oils used for this work. The reasons for this are varied, but perhaps one of the most important is the inherent film boiling properties that seem to be exhibited by FAME and its blends. This was further complicated by the varying viscosities exhibited by the blends.

Most conventional cooling processes involving vaporizable quenchants possess four cooling mechanisms: (1) shock boiling, (2) film boiling, (3) nucleate boiling, and (4) convection cooling processes. Since the ASTM D6200 standard 12.5-mm-dia × 60-mm cylindrical Inconel 600 probe provides cooling rate and temperature versus time at the core of probe, it is only possible to evaluate “average effective heat transfer coefficients” which are used in the heat treating industry. During quenching, the heat transfer coefficient is dependent on surface temperature of the steel part (probe) and mass and flow velocity of the quenchant. The variation of the heat transfer coefficient during film boiling is sufficiently small to permit the use of average values (α). During nucleate boiling and convective cooling, average effective heat transfer coefficients can be determined. In this paper, heat transfer coefficients were calculated according to the theory of regular conditions and the

calculation procedure described previously by Kobasko et al. (Ref 17) was used and will not be discussed further here.

3.3 Calculation of Heat Transfer Coefficients

Heat transfer processes are complex and the heat transfer coefficient is a complex function of variables describing this process. Generally, the heat transfer coefficient is a function of the fluid flow, component (probe) shape and dimensions, temperature, and physical properties of the liquid: thermal conductivity, specific heat capacity, density, and viscosity. The heat transfer coefficient can be defined as the quantity of heat transferred per unit time per unit area of a surface when the difference of temperatures between the surface and liquid equals one degree absolute. Since quenching processes are actually heat transfer processes; the heat transfer coefficient is an excellent single parameter for quenchant characterization.

In this work, the commercial code HT-MOD* (heat treating modeling) (Ref 18) was used to simulate the heat treatment process. This code is also used to calculate heat transfer coefficients as function of time by solving an inverse heat transfer problem. The model is based on a numerical optimization algorithm which includes a finite element module for calculating, with respect to time and space, the temperature distribution and its coupled microstructural evolution. In this case, since an Inconel 600 probe was used that does not undergo microstructural phase transformation, the differential problem solved is only the heat conduction Eq 1 in a cylindrical probe:

$$\nabla \cdot (k(\vec{r}, T) \cdot \nabla T) = c(\vec{r}, T)\rho(\vec{r}, T) \frac{\partial T}{\partial t} \quad (\text{Eq 1})$$

where $k(\vec{r}, T)$, $c(\vec{r}, T)$, and $\rho(\vec{r}, T)$ denote the thermal conductivity, the specific heat, and the density, respectively, of the material as dependent on the position (\vec{r}) and temperature T . $T(\vec{r}, t)$ is subjected to the initial condition

$$T(\vec{r}, t = 0) = T_0(\vec{r}); \quad \vec{r} \in \Omega \quad (\text{Eq 2})$$

and the following boundary conditions at the surface of the steel probe:

$$-k \frac{\partial T}{\partial n} = h_i(T - T_{\text{qu}}) \quad \text{on } \Gamma_i, \quad i = 1, \dots, p \quad (\text{Eq 3})$$

where $h_i(T)$ is the heat transfer coefficient corresponding to different portions of the boundary, Γ , and T_{qu} is the quenchant temperature. Each one of these p cooling zones has a time-dependent heat transfer coefficient that varies strongly along each partial boundary, depending on the heat transfer mechanism (vapor blanket, nucleate boiling, and convective cooling) that governs the energy flow.

Provided that the temperature change inside the component and on its surface is measured, it is possible to solve the inverse heat transfer problem to determine the time variation of the heat transfer coefficients, which best satisfies production demands. The time dependence of the heat transfer coefficient can be approximated by polygonal functions, each one defined by a set of parameters $h_i^{(r)}(r = 1, \dots, p; \quad i = 1, \dots, q)$.

On calling T_k^m the measured temperature and T_k^c the numerically calculated temperature at those points, one can pose the problem of obtaining the values of the heat transfer coefficients h_i that minimize the function:

$$S = S(h_i^{(r)}) = \sum_{k=1}^n (T_k^m - T_k^c)^2 = \min \quad (\text{Eq 4})$$

n being the total number of measured temperatures, i.e., the number of points times the number of measurements at each point.

The selection of the initial values for these coefficients and of the quantity and length of the time intervals was sample dependent. The time interval used to estimate the heat transfer coefficient was 0.4-0.6 s. The mean square difference between the measured and calculated temperatures obtained after optimization of the heat transfer coefficients was about 1 °C. Table 4 summarizes the thermo-physical properties INCONEL 600 used for this work (Ref 19).

3.4 Summary of Heat Transfer Coefficient Calculation Results

The calculated heat transfer coefficients as a function of cooling time and as a function of mean surface temperature for each of the fluids in Table 3 are shown in Fig. 6 and 7. Once again, it is important to note that the fluid viscosity at 40 °C for TEMP 2 is 16.96 cSt and is substantially lower than the 40 °C for TEMP 4 which is 52.86 cSt. Based on the fluid viscosities alone, the maximum heat transfer coefficient for TEMP 2 would be expected to be greater than that of TEMP 4 which was, in fact, observed. The film boiling region for TEMP 2 was significantly longer than that exhibited for TEMP 4, which was not expected since fast (accelerated) petroleum oil quenchants are typically formulated with additives to destabilize film boiling behavior. However, these data suggest that the terms “FAST” and “SLOW” are more reflective of the maximum heat transfer rate and fluid viscosity than behavior induced by additives.

For SO, an apparent film boiling region was observed, but was considerable shorter than the petroleum oil quenchant designated as TEMP 4. The maximum heat transfer coefficient was intermediate between that observed for the two petroleum oils: TEMP 2 and TEMP 4. The maximum heat transfer

Table 4 Temperature-dependent thermo-physical values for INCONEL 600 (Ref 19)

Thermal conductivity		Specific heat		Density	
Temp, °C	K , W/m K	Temp, °C	c , J/kg K	Temp, °C	ρ , kg/m ³
50	13.4	50	451	20	8400
100	14.2	100	467	100	8370
150	15.1	200	491	200	8340
200	16.0	300	509	300	8300
250	16.9	400	522	400	8270
300	17.8	500	533	500	8230
350	18.7	600	591	600	8190
400	19.7	700	597	700	8150
450	20.7	800	602	800	8100
500	21.7	900	611	900	8060
700	25.9				
900	30.1				

*HT-MOD is a commercial code which is available from KB Engineering S.R.L.; Florida 274, Piso 3, Of. 35 (1005) Buenos Aires, Argentina; Tel: 54-11 4326-7542; Fax: 54-11 4326-2424; Internet: <http://www.kbeng.com.ar>.

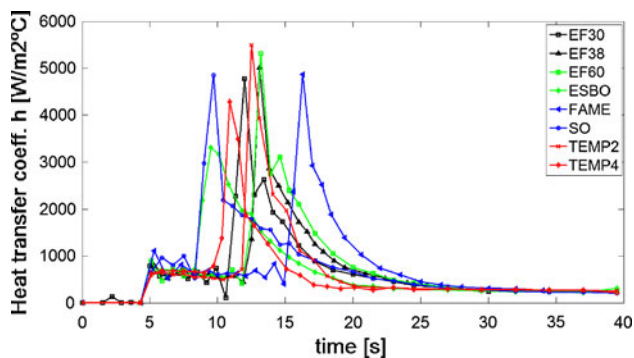


Fig. 6 Heat transfer coefficients' data at 60 °C bath temperature with no agitation as function of time

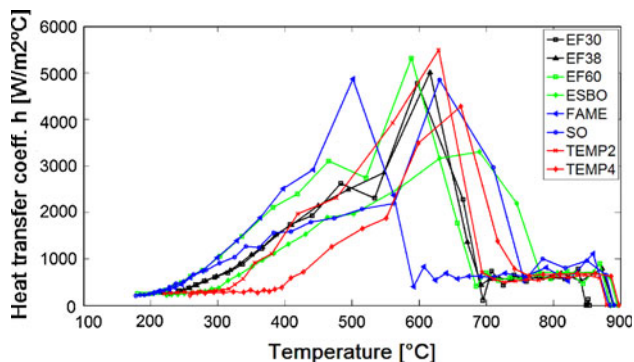


Fig. 7 Heat transfer coefficients' data at 60 °C bath temperature with no agitation as function of surface temperature

coefficient for SO occurred at approximately the same surface temperature as TEMP 4, but at a faster cooling time.

Comparing heat transfer coefficients exhibited by SO with ESBO during quenching showed that ESBO exhibited the same apparent film boiling behavior as SO, but the maximum heat transfer coefficient was much lower than either petroleum oil or SO. In addition, the maximum heat transfer coefficient occurred at the highest surface temperature of the fluids evaluated.

Although the maximum heat transfer coefficient for FAME was comparable to that obtained for SO, the total duration of the full-film boiling region was much longer than either SO or any of the ESBO/FAME blends. In addition, the maximum heat transfer coefficient occurred at a surface temperature substantially lower than either petroleum oil, SO, or ESBO.

EF 30, EF 38, and EF 60 are blends of ESBO and 30, 38, and 60% FAME, respectively. Interestingly, while there are some differences in these data, they tend not to be large. The cooling profiles, as indicated by the heat transfer coefficients, are dominated by the presence of FAME by exhibiting substantial durations of film boiling behavior and somewhat lower surface temperatures where the maximum heat transfer coefficients are obtained. Not surprisingly, EF 30 and EF 38 exhibited similar maximum heat transfer coefficients with respect to each other and to FAME and slightly less than that value exhibited by EF 60. However, further work may show that these differences are not significant. In all cases, the cooling behavior of these blends appears to be most similar to the TEMP2 petroleum oil quenchant than either ESBO or SO.

4. Conclusion

SO, EBSO, FAME, and blends of ESBO containing 30, 38, and 60% of FAME were prepared and the viscosity properties determined and cooling curve analysis performed using the ASTM D6200 test procedure. For comparison, two fully formulated, commercially available, petroleum-based “fast” and “slow” quench oils were also studied. The very high viscosity of ESBO would preclude its use as a quench oil due to excessive drag out. Therefore, the potential use of FAME derived from SO to reduce the viscosity of ESBO to model a petroleum oil-based quenchant was evaluated. The data obtained showed that the viscosity of ESBO was much more sensitive to temperature than either SO or FAME. Increasing amounts of FAME in the ESBO/FAME blend resulted in progressively less sensitivity of viscosity change relative to ESBO. The viscosity of the fast petroleum oil quenchant was more sensitive to temperature change than the slow petroleum oil quenchants, showing that it is formulated using a different petroleum oil basestock.

The quenching performance of SO suggests that heat transfer occurs predominantly by convection as does ESBO. However, FAME exhibits a prolonged film boiling region, suggesting that heat transfer occurs by three mechanisms: film boiling, nucleate boiling, and convection. The addition of FAME to ESBO imparts these characteristic heat transfer mechanisms to the overall cooling process and the duration of the film boiling region of the ESBO/FAME blends is relatively insensitive to the amount of FAME in the blend.

The characteristic film boiling process that typically accompanies petroleum oil-derived quenchants was not so clearly evident with the two petroleum oils evaluated here. This is most likely due to two factors. The first is that temperature change is measure in the center of the probe, whereas heat transfer is controlled by the mechanism of the interfacial cooling process at the surface. Therefore, the probe may not be sufficiently sensitive to observe the short-lived cooling process exhibited by these petroleum oils. The second reason is that it is likely that both petroleum oils contain additive(s) to either eliminate or reduce the duration of film boiling. Since the ESBO/FAME blends did not contain such additives, it was not possible, from the work conducted thus far, to conclude if the overall cooling process equivalent to these two particular petroleum oil quenchants is possible. This will be the subject of further work.

Acknowledgments

The authors gratefully acknowledge Inbra (Indústrias Químicas Ltda), Cognis Brasil Ltda, and Quimifort Indústria e Comércio Ltda. for donating the ESBO, FAME, and mineral oil quenchant fluids, respectively, and Tecumseh do Brasil Ltda for allowing the use of their Chemical Laboratory for viscosity measurements. The authors also acknowledge CAPES—Coordenação de Aperfeiçoamento de Pessoal de Nível Superior and Universidade de São Paulo (USP).

References

1. A. Adhvaryu and S.Z. Erhan, Epoxidized Soybean Oil as a Potential Source of High-Temperature Lubricants, *Ind. Crops Prod.*, 2002, **15**, p 247–254

2. R. Goyan, R.E. Melley, P.A. Wissner, and W.C. Ong, Biodegradable Lubricants, *Lubr. Eng.*, 1998, **54**(7), p 10–17
3. A. Zeeman, A. Sprengel, D. Niedermeier, and M. Späth, Biodegradable Lubricants—Studies of Thermo-Oxidation of Metal-Working and Hydraulic Fluids by Differential Scanning Calorimetry, *Thermochim. Acta*, 1995, **268**, p 9–15
4. C.W. Ruger, E.J. Klinker, and E.G. Hammond, Abilities of Some Antioxidants to Stabilize Soybean Oil in Industrial Use Conditions, *J. Am. Oil. Chem. Soc.*, 2002, **79**(7), p 733–736
5. A. Adhvaryu, S.Z. Erhan, Z.S. Liu, and J.M. Perez, Oxidation Kinetic Studies of Oils Derived from Unmodified and Genetically Modified Vegetables Using Pressurized Differential Scanning Calorimetry and Nuclear Magnetic Resonance Spectroscopy, *Thermochim. Acta*, 2000, **364**, p 87–97
6. M. Schneider, *Government Industry Forum on Non-Food Uses of Crops (GFGNFG 7/7), (2002)—Case Study: Plant Oil Based Lubricants in Total Loss and Potential Loss Applications*, Final Report Prepared for P. Smith, Network Manager, University of York, 2002
7. D.R. Kodali, High-Performance Ester Lubricants from Natural Oils, *Ind. Lubr. Tribol.*, 2002, **54**(4), p 165–170
8. G. Knothe, Dependence of Biodiesel Fuel Properties on the Structure of Fatty Acid Alkyl Esters, *Fuel Process. Technol.*, 2005, **86**, p 1059–1070
9. E.C. Souza, L.C.F. Canale, and G.E. Totten, Vegetable Oil Structure and Antioxidants, *Conference Proceedings of New Challenges in Heat Treating and Surface Engineering—Conference in Honor of Božidar Liščić*, June 9–12, Cavtat, Croatia, Croatian Society for Heat Treatment and Surface Engineering, Zagreb, 2009, p 45–52
10. H. Hwang and S.Z. Erhan, Synthetic Lubricant Basestocks from Epoxidized Soybean Oil and Guerbet Alcohols, *Ind. Crops Prod.*, 2006, **23**, p 311–317
11. P.L. Julian, H.T. Iveson, and S.B. Radlove, Hydroxylation of Vegetable Oils and Products Thereof, U.S. Patent 2,752,376, 1956
12. T.W. Findley, J.L. Ohlson, and F.E. Kuester, Treatment of Epoxy Fatty Compositions, U.S. Patent 3,035,069, 1962
13. X. Wu, X. Zhang, S. Yang, H. Chen, and D. Wang, The Study of Epoxidized Rapeseed Oil Used as a Potential Biodegradable Lubricant, *J. Am. Oil. Chem. Soc.*, 2000, **77**(5), p 561–563
14. S.Z. Erhan, A. Adhvaryu, and Z. Liu, Chemically Modified Vegetable Oil-Based Industrial Fluid, U.S. Patent 6,583,302 B1, 2003
15. J.C.O. Santos, I.M.G. Santos, and A.G. Souza, Effect of Heating and Cooling on Rheological Parameters of Edible Vegetable Oils, *J. Food Eng.*, 2005, **67**, p 401–405
16. K.M. Doll, B.K. Sharma, and S.Z. Erhan, Friction Reducing Properties and Stability of Epoxidized Oleochemicals, *Clean*, 2008, **36**(8), p 700–705
17. N.I. Kobasko, E. Carvalho de Souza, L.C.F. Canale, and G.E. Totten, Vegetable Oil Quenchants: Calculation and Comparison of the Cooling Properties of a Series of Vegetable Oils, *Strojniški vestnik—J. Mech. Eng.*, 2010, **56**(2), p 131–142
18. G.S. Sarmiento, A. Gastón, and J. Vega, Inverse Heat Conduction Coupled with Phase Transformation Problems in Heat Treating Process, *Computational Mechanics—New Trends and Applications*, E. Oñate and S.R. Idelsohn, Eds., CIMNE, Barcelona, 1998, CD Book, Part VI, Section 1, Paper 16
19. J. Clark and R. Tye, Thermophysical Properties Reference Data for Some Key Engineering Alloys, *High Temp.—High Press.*, 2003/2004, **35/36**, p 1–14